FreeDetector: Device-Free Occupancy Detection with Commodity WiFi

Han Zou[1], Yuxun Zhou[1], Jianfei Yang[2], Weixi Gu[3], Lihua Xie[2] and Costas Spanos[1]
[1] Department of Electrical Engineering and Computer Sciences, University of California, Berkeley, USA
[2] School of Electrical and Electronics Engineering, Nanyang Technological University, Singapore
[3] Tsinghua-Berkeley Shenzhen Institute, Tsinghua University, China
Email: {$hanzou, yxzhou, spanos$}@berkeley.edu, {$yang0478, elhxie$}@ntu.edu.sg, guweixigavin@gmail.com

***Abstract*—Occupancy detection is playing a critical role to improve the efficiency of building management system and optimize personalized thermal comfort, among many other emerging applications. Conventional occupancy detection methods, such as Passive Infra-Red (PIR) and camera, have several drawbacks including low accuracy, high intrusiveness and extra infrastructure. In this work, we propose FreeDetector, a device-free occupancy detection scheme that is able to detect human presence accurately just using existing commodity WiFi routers. We upgrade the firmware of the routers so that the channel state information (CSI) data in PHY layer can be obtained directly from them. With only two routers, FreeDetector is able to reveal the variations in CSI data caused by human presence. We leverage signal tendency index (STI) to analyze the shape similarity of adjacent time series CSI curves. The most representative subset of subcarriers is selected by greedy algorithm and we utilize machine learning algorithm to construct a detection classifier. Extensive experiments are conducted and the results demonstrate that FreeDetector is able to provide outstanding occupancy detection service in terms of both accuracy and efficiency.**

I. Introduction

Precise detection of occupant presence is essential and crucial to improve the efficiency of building management system (BMS) and optimize occupant's thermal comfort in buildings. Occupancy detection also plays a central role in various applications, such as patient monitoring in hospital, children and elderly monitoring at home and intrusion detection in office [1]–[5], and demand response in power systems [6], [7]. Traditional techniques for occupancy detection include Passive Infra-Red (PIR) [8], RFID [9], vision [10], Bluetooth [11] and environmental sensors [12]. PIR, RFID, Bluetooth and environmental sensors require extra infrastructure. Vision based approaches cause privacy concerns and require satisfactory lighting conditions. Thus, a cost-effective, device-free and non-intrusive scheme for pervasive occupancy detection is urgently desired.

With the pervasive availability of WiFi infrastructure in both residential and commercial buildings, WiFi has become the primary sensing technique for indoor localization [13]–[15]. Various WiFi based indoor positioning systems have been proposed in recent years [16]–[18]. Furthermore, device-free occupancy detection can be realized by observing the variations of WiFi signal caused by human body. One straightforward method to infer the human presence is exploiting the Received Signal Strength (RSS) variations at MAC layer, which can be easily accessed from Commercial Off-The-Shelf (COTS) WiFi routers. However, its detection accuracy is usually poor because RSS is a coarse measurement which fails to capture the multipath effects caused by occupants [19]. Alternatively, fine-grained measurement at PHY layer is more sensitive to the presence of occupant and more robust to background noise. As a subcarrier-level channel measurement at PHY layer, Channel State Information (CSI) offers exquisite channel description at the granularity of Frequency Division Multiplexing (OFDM) subcarriers [19]. It is able to capture small-scale multipath propagation of WiFi signal from transmitter (TX) to receiver (RX) over multiple subcarriers, that reveals various influences of occupants on the physical qualities of the channel, e.g., shadowing, scattering and frequency selective fading.

In this paper, we propose FreeDetector, a device-free occupancy detection scheme that could detect the presence of occupant precisely using commodity WiFi routers. We observed that the shapes of unoccupied CSI measurements' curves are smooth and display certain similarities, while the variations of the curves of occupied readings are much higher. This observation motivates us to measure the shape similarity between adjacent time series CSI curves using signal tendency index (STI) [20], and employ it as an index for device-free occupancy detection. Meanwhile, in order to select the most representative subset of subcarriers for occupancy detection while reducing the computational overhead, we formulate this issue as an optimization problem and propose greedy algorithm to solve it. Finally, with STI data from the optimal subset of subcarriers, we apply machine learning algorithms and choose random forest to train a robust classifier to capture the event of human presence. To implement FreeDetector on COTS WiFi routers directly instead of using laptop with external WiFi NIC card, we upgrade the Atheros CSI Tool [21] and develop a new OpenWrt based firmware for the routers so that the CSI measurements can be obtained directly from them. We prototype FreeDetector on COTS WiFi routers and conduct extensive experiments in typical indoor environments for performance validation. In a nutshell, FreeDetector outperforms is able to realize device-free occupancy detection with 94% accuracy in a reliable and efficient manner.

The rest of the paper is organized as follows. Section II introduces the detailed system design of FreeDetector. In Section III, the experiment procedure is elaborated and the

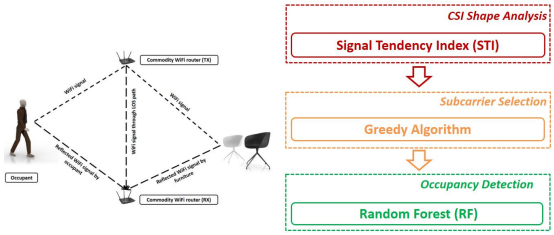

Fig. 1. System architecture of FreeDetector.

results are analyzed. We conclude the work in Section IV.

II. System Design

The overall objective of FreeDetector is to detect the presence of occupant in a non-intrusive manner using COTS WiFi routers. In this section, we introduce preliminaries of CSI firstly. Then, the CSI data acquisition platform is illustrated. After that, as shown in Fig. 1, we present the methodology of FreeDetector, including shape analysis of time series CSI data, subcarrier selection using greedy algorithm and occupancy detection by random forest.

A. Channel State Information

In typical indoor environment, WiFi signal propagates through multiple paths from TX to RX due to reflection, scattering and diffraction introduced by furniture and occupants [19]. Nowadays, most of COTS WiFi devices are equipped with multiple antennas for multiple input, multiple output (MIMO) communication and adopt OFDM in PHY layer that supports IEEE 802.11n/ac standard. Thus, different from the RSS from MAC layer which only represents the superimposition of multipath signals, by monitoring the frequency response of OFDM subcarriers continuously, CSI reveals the fine-grained information (both magnitude and phase) of each subcarrier when the signal travels between each transmitter-receiver antenna pair [19].

The WiFi signal can be modeled as Channel Impulse Response (CIR) $h(\tau)$ to discriminate individual paths in time domain, $h(\tau) = \sum_{i=0}^{M-1} a_i e^{-j\theta_i} \delta(\tau - \tau_i)$ where a_i, θ_i and τ represent the amplitude, phase and time delay of the i^{th} path respectively, M indicates the total number of paths and $\delta(\tau)$ is the Dirac delta function. Nevertheless, due to the limited bandwidth of WiFi (40 MHz for 5 GHz band), only clusters of multipath components can be distinguished. On the other hand, in frequency domain, OFDM receiver is able to provide a sampled version of the signal spectrum of each subcarrier, which contains both amplitude attenuation and phase shift as complex numbers. These measurements can be revealed to upper layer in the format of CSI $H_k = \|H_k\| e^{j\angle H_k}$, where $\|H_k\|$ and $\angle H_k$ denote the amplitude and the phase of the CSI at the k^{th} subcarrier respectively.

B. CSI Data Acquisition from Commodity WiFi Router

Conventional CSI-based indoor localization and sensing systems adopt either Intel 5300 NIC tool [22] or Atheros 9390 tool [23] as the platform. These systems require a laptop or PC, which is equipped with an additional WiFi NIC card, as the receiver. This excessive demand of infrastructure severely hinders them for large-scale implementation. For instance, 11 laptops are utilized to serve as receivers for fine-grained indoor localization in [24]. Thus, to overcome this bottleneck, we upgrade the Atheros CSI Tool [21] and develop a new OpenWrt based firmware for commodity WiFi routers so that the CSI measurements can be obtained directly from them and enable them as receiver instead of using laptop or PC with external WiFi NIC adapter. Moreover, our platform reports CSI data of 114 subcarriers for 40 MHz bandwidth for each TX-RX pair when both TX and RX routers operate on 5 GHz, which provides much more information than conventional CSI tools (only reports data from 30 subcarriers). FreeDetector only needs two routers, one serves as TX and the other is adopted as RX, to perform device-free occupancy detection. TX continuously transmits data packets and RX monitors the channels, captures and analyzes these packets. We observed that the event of human presence increases the fluctuation of CSI readings when the occupant is near or crossing the LOS between TX and RX. Thus, we aim to leverage this phenomenon to infer occupancy. Suppose N_{TX} and N_{RX} represent the number of transmit and receive antennas. At each time instant, $N_{TX} \times N_{RX} \times 114$ CSI streams are available for us to analyze the variations of WiFi communication links caused by human presence.

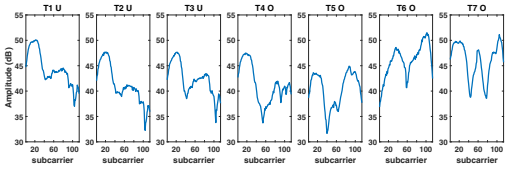

Fig. 2. Curves of CSI values from unoccupied to occupied scenarios.

C. Shape Similarity of Time Series CSI Curves

Fig. 2 depicts the CSI values of all the 114 subcarriers in a TX-RX pair for 7 continuous timestamps when the environmental status changes from unoccupied (U: from T1 to T3) to occupied (O: from T4 to T7). It can be observed from Fig. 2 that there are obviously difference between unoccupied and occupied CSI samples.

One key insight we observed from Fig. 2 is that the shapes of unoccupied samples' curves are smooth and display certain similarities, while the variations of the occupied samples are much higher. It is reasonable because when an occupant is passing through the TX-RX pairs, the WiFi signals reflected by human body travel through a different path, which leads to severe distortion of the CSI values. On the other hand, the shapes of CSI curves under unoccupied situations are similar because the environment is more stable.

This observation indicates that the shape similarity between adjacent CSI curves in time series can be employed as an index for device-free occupancy detection. Therefore, we utilize signal tendency index (STI) [20], which is based on Procrustes analysis, to compare the shape similarity of CSI

$$\min_{X\subseteq V} \mathrm{J} = \left| \frac{1}{N_u}\sum_{j=1}^{N_u} S_j^u(X) - \frac{1}{N_o}\sum_{i=1}^{N_o} S_i^o(X) \right| + \lambda_o \sqrt{\frac{1}{N_o}\sum_{i=1}^{N_o}\left(S_i^o(X) - \overline{S^o(X)}\right)} + \lambda_u \sqrt{\frac{1}{N_u}\sum_{j=1}^{N_u}\left(S_j^u(X) - \overline{S^o(X)}\right)} \quad (2)$$

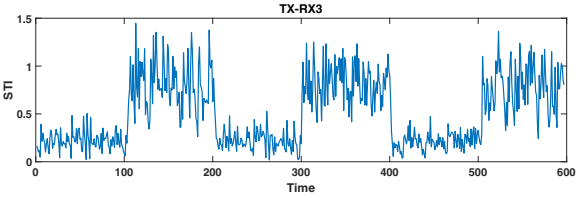

Fig. 3. STI values of one TX-RX pair.

curves. STI 'superimposes' these curves by optimally translating and uniformly scaling. Suppose $H_1^t, H_2^t, \ldots, H_n^t$ is the CSI vector at timestamp t. The translation setup will produce $H_1^t - \overline{H^t}, H_2^t - \overline{H^t}, ..., H_n^t - \overline{H^t}$, where $\overline{H^t} = \frac{1}{n}\sum_{j=1}^{n} H_j^t$. Then, in the uniformly scaling step, we have

$$\widehat{H^t} = [H_1^t - \overline{H^t}, H_2^t - \overline{H^t}, ..., H_n^t - \overline{H^t}]/\sigma(H^t), \quad (1)$$

where $\sigma(\hat{H}^t) = \sqrt{\frac{1}{n}\sum_{j=1}^{n}(H_j^t - \overline{H^t})^2}$. The vector $\widehat{H^t}$ is thus the transformed object for the CSI curves at t. The CSI data at the previous timestamp $t-1$ can be derived easily in the same manner. To evaluate the similarity between the two adjacent CSI curves in terms of their shapes, STI is computed as $S = \|\widehat{H^t} - \widehat{H^{t-1}}\|$ where $\|\cdot\|$ denotes the Euclidean norm. Small S indicates that the shapes of two curves are close to each other, while large S means they are uncorrelated. Fig. 3 demonstrates the calculated STI values of one TX-RX pair where the ground truths of occupied samples are timestamps [101-200, 301-400, 501-600] and the others are unoccupied scenario. It can be observed that the STI values under unoccupied situations are kept in a low level while the STI values in occupied scenario are much higher. This primary result validates our assumption that the shape similarity between adjacent time series CSI curves is a potential index to infer human presence.

D. Subcarrier Selection

Another observation we made from the experiment is that the human presence does not affect CSI measurements of every subcarrier equally. Meanwhile, as demonstrated in Fig. 3, the STI value becomes smaller during occupied situations sometimes, which are close to those values in unoccupied situations. In this case, fault detection will be introduced if a hard threshold method is adopted to determine the occupancy status. We formulate the subcarrier selection problem as an optimization problem. During the training phase, after calculating the STI values of the collected occupied and unoccupied CSI samples, we aim to maximize the gap between the means of STI for occupied and unoccupied samples so we could easily distinguish the occupancy status, and minimize the standard deviations of STI for both occupied and unoccupied samples to make our detection scheme robust and stable. The objective function is formulated as Equation (2),

where X indicates a subcarrier and V is the universal set of all subcarriers, N_u and S^u denote the number of unoccupied samples and their STI values, N_o and S^o denote the number of occupied samples and their STI values, λ_u and λ_o represent the weights for the standard deviations of unoccupied and occupied STI values. We employ greedy algorithm to solve the aforementioned optimization problem. The essence of greedy algorithm is to make a local optimal choice at each stage with the hope of approximating the global optimum. Furthermore, it has been proven in [25] that greedy strategy is able to produce a near optimal solution to the original NP-hard problem [26]. The methodology of greedy algorithm for subcarrier selection is illustrated in Algorithm 1. Initially, the optimal subset of subcarriers is an empty subset A_0. Then, at each step k, the greedy algorithm selects one subcarrier that achieves the best marginal improvement and put it into the subset $A_k \leftarrow A_{k-1} \cup X_k$. In this manner, the optimal subset of subcarriers that minimize the objective function are selected for occupancy detection eventually.

E. Occupancy Detection based on Random Forest

By leveraging the STI values from the selected subcarriers, we aim to develop a robust classifier to detect the presence of occupant. Most of existing works adopt simple hard threshold-based methods for occupancy detection, which rely on scenario-tailored calibration and the calibrated thresholds may not perform well consistently in various environment [27]. To overcome this issue, we applied various machine learning based approaches [28]–[31] and found that random forest (RF) provides the best performance in terms of both accuracy and efficiency. As an ensemble learning method, the rationale for RF is constructing a multitude of decision trees during the training phase and output the mode of classes of the individual trees for prediction. To avoid correlation among base trees, random set of features are selected in the splitting process when constructing each decision tree.

We formulate the occupancy detection problem as a binary classification problem (occupied or unoccupied), and leverage the conditional inference tree algorithm to solve it. Suppose N STI samples were collected for training. For each sample, the inputs are the calculated STI values from N_{RX} antennas which can be represented as $[\mathbf{S} = S_1, S_2, \ldots, S_{N_{RX}}]$, and the training target $Y = u \| o$ is the occupancy. Each decision tree is grown as follows: 1) construct a training set for the tree by choosing n times with replacement from all N available STI training samples; 2) the rest of the samples are used to estimate the error of the tree by predicting their classes; 3) at each node of the tree, m variables (RX antennas) are chosen based on which the decision is made at that node. Then, the best split based on these m variables in the training set is calculated; 4) Each tree is fully grown and not pruned.

Algorithm 1 Greedy algorithm for subcarrier selection

$A_0 \leftarrow \phi$

for $k = 1, \ldots, m$ **do**

$$X_k = \arg\min_{y \in V \setminus A_{k-1}} \left| \frac{1}{N_u} \sum_{j=1}^{N_u} S_j^u(A_{k-1} \cup y) - \frac{1}{N_o} \sum_{i=1}^{N_o} S_i^o(A_{k-1} \cup y) \right| + \lambda_o \sqrt{\frac{1}{N_o} \sum_{i=1}^{N_o} \left(S_i^o(A_{k-1} \cup y) - \overline{S^o(A_{k-1} \cup y)} \right)} + \lambda_u \sqrt{\frac{1}{N_u} \sum_{j=1}^{N_u} \left(S_j^u(A_{k-1} \cup y) - \overline{S^o(A_{k-1} \cup y)} \right)}$$

$A_k \leftarrow A_{k-1} \cup X_k$

end for

Fig. 4. System setup of FreeDetector.

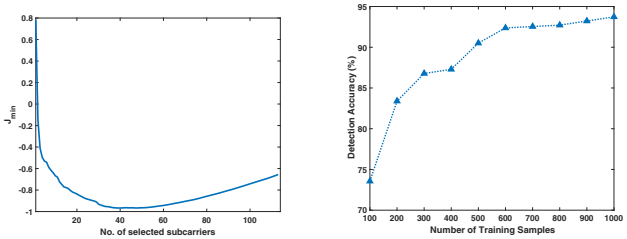

(a) (b)

Fig. 5. (a)Subcarrier selection, (b)Impact of the size of training set.

When new CSI measurements are obtained, the calculated STI values of these data are used as input for each tree, each tree estimates the occupancy status and the final estimation of RF is the majority results of all trees.

III. Implementation and Evaluation

In this section, we interpret the experiment methodology firstly, followed by the detailed performance evaluation.

1) Experimental Setup and Data Collection: We implemented a prototype of FreeDetector on two TPLINK N750 wireless dual band routers: one serves as TX and another one acts as RX. We upgraded their firmware to our Atheros CSI OpenWrt version as introduced in Section II-B, so that the CSI readings from PHY layer can be reported directly from them instead of additional setup of laptop with external WiFi NIC adapter. TX operated in 802.11n AP mode at 5 GHz with a 40 MHz bandwidth and RX connected to the TX's network wirelessly in client mode. We used one antenna of TX ($N_{TX} = 1$) to send data packets to the RX with 3 antennas ($N_{RX} = 3$) at a transmission rate of 30 Hz. At each time instant, $1 \times 3 \times 114$ CSI streams were captured for data analysis. The experiments were conducted in a typical conference room. As shown in Fig. 4, two routers were 5 meters apart and placed on tripods at height of 1.4 meters. Other WiFi networks such as campus network were operated as usual during the entire experiments.

We conducted 3 set of experiments with different environmental scenarios: 1) unoccupied room for 20s, 2) one occupant was continuously walking through the LOS link between TX and RX causally for 20s, 3) the same occupant was walking through the LOS link for 3s with an interval of 3s for 3 times. The CSI data collected from experiment 1) and 2) were utilized as training dataset for subcarrier selection and RF modeling. Data obtained in experiment 3) were employed as testing dataset for performance evaluation.

2) Subcarrier Selection: We evaluated the performance of the proposed subcarrier selection scheme. Fig. 5(a) depicts the minimum value of the objective function J when different number of subcarriers are chosen. As shown in Fig. 5(a), J becomes smaller when more subcarriers are selected at the beginning. The overall minimum of J is achieved when 39 subcarriers are selected. After that, the value of J increases when more subcarriers are added in the subset. The intuition of these is that the newly selected subcarriers provide redundant information for occupancy detection. Therefore, in order to achieve the optimal performance and reduce the computational overhead, we only make use of the 39 subcarriers that achieved J_{min} as the input for the RF occupancy detection scheme.

3) Occupancy Detection Accuracy: By using the STI values obtained from the selected subcarriers, the classification model is constructed using RF as introduced in Section II-E. FreeDetector achieves 93.73% occupancy detection accuracy (corrected detected samples/all the samples). It is able to precisely detect 95.52% and 92% of occupied and unoccupied events respectively.

4) Impact of Training Data Size: The impact of the number of training samples on the detection accuracy is also evaluated. As presented in Fig. 5(b), the accuracy increases when more training samples are leveraged. The performance becomes stable around 93% when 700 training samples or more are utilized. Since the sampling rate of FreeDetector is 30 samples/s, 12s of occupied and unoccupied training samples are sufficient to enable it to provide reliable occupancy detection service.

IV. Conclusion

In this paper, we proposed FreeDetector, a device-free occupancy detection scheme that is able to detect the presence of occupant accurately with commodity WiFi routers. We developed a novel OpenWrt based firmware for COTS WiFi routers so that the CSI measurements in PHY layer can be obtained directly from them instead of using laptop with an external WiFi NIC card. Only two COTS WiFi routers are required for FreeDetector to be functional. STI was adopted to analyze the shape similarity of adjacent time series CSI curves. After that, we leveraged greedy algorithm to select the most representative subset of subcarriers for occupancy detection and reduction of computational cost. We utilized RF to construct a reliable classifier to detect human presence. We prototyped FreeDetector on COTS WiFi routers and the experimental results have validated that it can provide outstanding occupancy detection service in terms both accuracy and efficiency.

Acknowledgement

This research is funded by the Republic of Singapore National Research Foundation (NRF) through a grant to the Berkeley Education Alliance for Research in Singapore (BEARS) for the Singapore-Berkeley Building Efficiency and Sustainability in the Tropics (SinBerBEST) Program. BEARS has been established by the University of California, Berkeley as a center for intellectual excellence in research and education in Singapore.

References

[1] Y. Zhou, *Statistical Learning for Sparse Sensing and Agile Operation*. PhD thesis, EECS Department, University of California, Berkeley, May 2017.

[2] W. Gu, "Non-intrusive blood glucose monitor by multi-task deep learning: Phd forum abstract," in *Proceedings of the 16th ACM/IEEE International Conference on Information Processing in Sensor Networks*, pp. 249–250, ACM, 2017.

[3] M. Jin, R. Jia, and C. Spanos, "Virtual occupancy sensing: Using smart meters to indicate your presence," *IEEE Transactions on Mobile Computing*, vol. 99, p. 1, 2017.

[4] Y. Zhou, R. Arghandeh, and C. J. Spanos, "Data-driven event detection with partial knowledge: A hidden structure semi-supervised learning method," in *American Control Conference (ACC16)*, IEEE, 2016.

[5] W. Gu, Z. Yang, L. Shangguan, W. Sun, K. Jin, and Y. Liu, "Intelligent sleep stage mining service with smartphones," in *Proceedings of the 2014 ACM International Joint Conference on Pervasive and Ubiquitous Computing*, pp. 649–660, ACM, 2014.

[6] Y. Zhou, R. Arghandeh, I. C. Konstantakopoulos, S. Abdullah, A. von Meier, and C. J. Spanos, "Abnormal event detection with high resolution micro-pmu measurement," in *IEEE Power Systems Computation Conference*, IEEE, 2016.

[7] Y. Zhou, R. Arghandeh, and C. J. Spanos, "Partial knowledge data-driven event detection for power distribution networks," *IEEE Transactions on Smart Grid*, 2017.

[8] Y. Agarwal, B. Balaji, S. Dutta, R. K. Gupta, and T. Weng, "Duty-cycling buildings aggressively: The next frontier in hvac control," in *Information Processing in Sensor Networks (IPSN), 2011 10th International Conference on*, pp. 246–257, IEEE, 2011.

[9] H. Zou, L. Xie, Q.-S. Jia, and H. Wang, "Platform and algorithm development for a rfid-based indoor positioning system," *Unmanned Systems*, vol. 2, no. 03, pp. 279–291, 2014.

[10] V. L. Erickson, M. Á. Carreira-Perpinán, and A. E. Cerpa, "Occupancy modeling and prediction for building energy management," *ACM Transactions on Sensor Networks (TOSN)*, vol. 10, no. 3, p. 42, 2014.

[11] H. Zou, H. Jiang, Y. Luo, J. Zhu, X. Lu, and L. Xie, "Bluedetect: An ibeacon-enabled scheme for accurate and energy-efficient indoor-outdoor detection and seamless location-based service," *Sensors*, 2016.

[12] M. Jin, H. Zou, K. Weekly, R. Jia, A. M. Bayen, and C. J. Spanos, "Environmental sensing by wearable device for indoor activity and location estimation," in *Industrial Electronics Society, IECON 2014-40th Annual Conference of the IEEE*, pp. 5369–5375, IEEE, 2014.

[13] D. Lymberopoulos, J. Liu, X. Yang, R. R. Choudhury, V. Handziski, and S. Sen, "A realistic evaluation and comparison of indoor location technologies: experiences and lessons learned," in *Proceedings of the 14th International Conference on Information Processing in Sensor Networks*, pp. 178–189, ACM, 2015.

[14] H. Zou, H. Jiang, X. Lu, and L. Xie, "An online sequential extreme learning machine approach to wifi based indoor positioning," in *2014 IEEE World Forum on Internet of Things (WF-IoT)*, pp. 111–116, IEEE, 2014.

[15] X. Lu, H. Zou, H. Zhou, L. Xie, and G.-B. Huang, "Robust extreme learning machine with its application to indoor positioning," *IEEE transactions on cybernetics*, vol. 46, no. 1, pp. 194–205, 2016.

[16] H. Zou, X. Lu, H. Jiang, and L. Xie, "A fast and precise indoor localization algorithm based on an online sequential extreme learning machine," *Sensors*, vol. 15, no. 1, pp. 1804–1824, 2015.

[17] Z. Chen, H. Zou, H. Jiang, Q. Zhu, Y. C. Soh, and L. Xie, "Fusion of wifi, smartphone sensors and landmarks using the kalman filter for indoor localization," *Sensors*, vol. 15, no. 1, pp. 715–732, 2015.

[18] H. Zou, M. Jin, H. Jiang, L. Xie, and C. Spanos, "Winips: Wifi-based non-intrusive ips for online radio map construction," in *2016 IEEE Conference on Computer Communications Workshops (INFOCOM WKSHPS)*, pp. 1081–1082, IEEE, 2016.

[19] Z. Yang, Z. Zhou, and Y. Liu, "From rssi to csi: Indoor localization via channel response," *ACM Computing Surveys (CSUR)*, vol. 46, no. 2, p. 25, 2013.

[20] H. Zou, B. Huang, X. Lu, H. Jiang, and L. Xie, "A robust indoor positioning system based on the procrustes analysis and weighted extreme learning machine," *Wireless Communications, IEEE Transactions on*, vol. 15, no. 2, pp. 1252–1266, 2016.

[21] Y. Xie, Z. Li, and M. Li, "Precise power delay profiling with commodity wifi," in *Proceedings of the 21st Annual International Conference on Mobile Computing and Networking*, pp. 53–64, ACM, 2015.

[22] D. Halperin, W. Hu, A. Sheth, and D. Wetherall, "Tool release: gathering 802.11 n traces with channel state information," *ACM SIGCOMM Computer Communication Review*, vol. 41, no. 1, pp. 53–53, 2011.

[23] S. Sen, J. Lee, K.-H. Kim, and P. Congdon, "Avoiding multipath to revive inbuilding wifi localization," in *Proceeding of the 11th annual international conference on Mobile systems, applications, and services*, pp. 249–262, ACM, 2013.

[24] J. Wang, H. Jiang, J. Xiong, K. Jamieson, X. Chen, D. Fang, and B. Xie, "Lifs: Low human effort, device-free localization with fine-grained subcarrier information," in *Proceedings of the 22nd Annual International Conference on Mobile Computing and Networking*, pp. 243–256, ACM, 2016.

[25] Y. Zhou and C. J. Spanos, "Causal meets submodular: Subset selection with directed information," in *Advances In Neural Information Processing Systems*, pp. 2649–2657, 2016.

[26] L. Dan, Y. Zhou, H. Guoqiang, and C. J. Spanos, "Optimal sensor configuration and feature selection for fault detection and diagnosis of air handling unit," *IEEE Transactions on Industrial Informatics*, 2016.

[27] C. Wu, Z. Yang, Z. Zhou, X. Liu, Y. Liu, and J. Cao, "Non-invasive detection of moving and stationary human with wifi," *IEEE Journal on Selected Areas in Communications*, vol. 33, no. 11, pp. 2329–2342, 2015.

[28] Y. Zhou, Z. Kang, and C. J. Spanos, "Parametric dual maximization for non-convex learning problems," in *Thirty-First AAAI Conference*, AAAI, 2017.

[29] Y. Zhou, H. Ninghang, and C. J. Spanos, "Veto-consensus multiple kernel learning," in *Thirtieth AAAI Conference*, AAAI, 2016.

[30] Y. Zhou, J. Baihong, and C. J. Spanos, "Learning convex piecewise linear machine for data-driving optimal control," in *Machine Learning and Applications (ICMLA), 2015 14th International Conference on*, pp. 171–177, IEEE, 2015.

[31] Y. Zhou, J. Y. Baek, D. Li, and C. J. Spanos, "Optimal training and efficient model selection for parameterized large margin learning," in *Advances in Knowledge Discovery and Data Mining: 20th Pacific-Asia Conference, PAKDD 2016*, 2016.